

Effective Field Theory for Compact Object Evolution in Non-Relativistic General Relativity

Irvin Martinez and Amanda Weltman
*High Energy Physics, Cosmology & Astrophysics Theory Group,
Department of Mathematics & Applied Mathematics,
University of Cape Town, Cape Town, 7701, South Africa*
(Dated: December 22, 2024)

We describe the evolution of slowly spinning compact objects in the late inspiral with Newtonian corrections due to spin, tides, dissipation and post-Newtonian corrections to the point mass term in the action within the effective field theory framework. We evolve the system numerically using a simple algorithm for point particle simulations and extract the lowest-order Newtonian gravitational waveform to study its phase evolution due to the different effects. We show that the matching of coefficients of the effective field theory for compact objects from systems that the gravitational wave observatories LIGO-Virgo currently detects might be possible and it can place tight constraints on fundamental physics.

I. INTRODUCTION

The astonishing firsts detection of gravitational waves (GW) by the LIGO-Virgo observatories from a binary black hole (BBH) merger [1] and from a binary neutron star merger [2] have opened up a new window to test fundamental physics in the strong regime of gravity, from which we now know properties of the compact objects better than before [3]. The era of precision gravity has arrived, and with it the potential for great discovery using multi-messenger astronomy to better understand the universe on all scales. On the theoretical side, the development of better tools to model the dynamics of any astrophysical source can only aid in this discovery.

In this work we bring the tools of effective field theory (EFT) to the study of astrophysics to model black holes (BHs) and neutron stars (NSs) using point particle simulations. We introduce a known methodology for simulating stellar dynamics as point particles [4] into the framework of EFTs for compact objects. The simulation solves the equations of motion at each time step for given initial conditions. From the EFT perspective the dynamics are obtained from an action of a point particle with higher order terms that correspond to corrections due to additional effects. Solving numerically for the point particle as well as for its additional effects, allows us to evolve the system with high accuracy for a cheap computational cost.

We start with an effective theory for a spinning extended object derived from the coset construction [5] and systematically include leading order Newtonian corrections due to spin, dynamical tides [6], dissipation [7, 8], and GW radiation using the 2.5 Post-Newtonian (PN) correction to the point mass term in the Non-Relativistic regime of General Relativity [9]. With these ingredients, we obtain the equations of motion and solve them numerically using a 4th order Hermite integrator. This powerful, fast and simple methodology of simulating a compact object as a point particle plus corrections allows us to study stellar interactions in the strong regime

of gravity without the need for numerical relativity [10], which is usually computationally expensive. The PN expansion encodes non-linearities of the theory of General Relativity and PN simulations match numerical relativity simulations with high accuracy up to a few orbits before the merger [11]. This numerical implementation goes beyond PN and systematically takes into account for the very first time dynamical tides and dissipative effects in the stellar model within the EFT framework, building up more realistic binaries. We also add aligned spin to some components of the binaries. In this sense, our results with state of the art of PN results will allow us to better model GW systems for GW extraction.

The role of these effects in the phase evolution of the gravitational waveform becomes relevant in the late inspiral. Thus, we run late inspiral simulations of systems in quasi-circular orbits until there is a collision or a disruption of a NS, to later extract the GWs and study the overall phase evolution due to the different effects. We test the code by introducing the matching of coefficients and matching them at each timestep of the simulation. The operators in the point particle action have coefficients which encapsulate the properties of the structure of the stellar objects. These coefficients are to be matched from experiments, like the coalescence of binary systems made up of compact objects.

We show that the phase evolution is significant for the different effects to possibly match the coefficients of the theory. In binaries with NSs, the matching of the coefficients from dynamical tides which has been computed in the EFT framework [6], can place tighter constraints on the equation of state of matter compared to only taking into account static tidal effects [12], given that as we show, the dynamical part plays an important role in the phase evolution and a deeper analysis needs to be done as in [13]. The matching of coefficients to black holes is a test to General Relativity. Dissipative effects in a BBH coalescence have a minor role in the phase evolution compared to tidal effects but they still have a significant contribution that is likely to be matched from an unequal mass case of systems that LIGO-Virgo currently detects,

in comparison with previous works on dissipative effects for LISA binaries [14, 15]. By successfully matching the coefficients for BHs and NSs from observations we can constrain fundamental physics, such as the equation of state of matter for neutron stars and the nature of gravity.

In section II we explain the effective action from the coset construction which systematically includes spin, finite-size and dissipative effects. Then take the Newtonian limit, derive the equations of motion and consider leading order GW radiation effects to the point mass term of the action. In section III we implement the formalism numerically using point particle simulations and measure the coefficients to test our implementation. We then quantify the effects in the gravitational waveform. In section IV we discuss the implications of the numerical results.

II. EFFECTIVE FIELD THEORY FOR STELLAR COMPACT OBJECTS

We start with an effective action for a slowly spinning star [5, 8]

$$\mathcal{S}_{eff} = \mathcal{S}_{PP} + \mathcal{S}_{\Omega} + \mathcal{S}_Q + \mathcal{S}_{\mathcal{O}} \quad (1)$$

where \mathcal{S}_{PP} is the the action for a point particle coupled to gravity, \mathcal{S}_{Ω} corrections due to spin, \mathcal{S}_Q dynamical tides and $\mathcal{S}_{\mathcal{O}}$ dissipative effects. We consider each of the leading order terms for these effects in turn, to see their overall role. Thus the effective action reads

$$\begin{aligned} \mathcal{S}_{eff} = \int d\tau \left\{ -mc^2 + \frac{I}{2} \tilde{\Omega}_i \tilde{\Omega}^i + \dots \right. \\ \left. + n_{\Omega} \tilde{\Omega}^i \tilde{\Omega}^j \tilde{C}_{0i0j} + \tilde{Q}_E^{ij} \tilde{C}_{0i0j} + \tilde{O}_E^{ij} \tilde{C}_{0i0j} + \dots \right\} \quad (2) \end{aligned}$$

The tildes represent the comoving frame. This action is Lorentz invariant and is compatible with all possible symmetries [8]. The first line describes the leading order corrections for a relativistic spinning particle with mass m , moment of inertia I and angular velocity $\tilde{\Omega}_i$. The third term is a spin correction due to gravity with \tilde{C}_{0i0j} the traceless Weyl tensor. The fourth term accounts for dynamical quadrupolar tidal effects [6] with $\tilde{Q}_E = \tilde{F}(\tau) \tilde{C}_{0i0j}$ and $\tilde{F}(\tau)$ a response function which Fourier transformation can be Taylor expanded as $\mathcal{F}(\tilde{F})(\tilde{\omega}) = n_E + n'_E \tilde{\omega}^2$ [16]. The coefficients n_E and n'_E are the Love numbers of the compact object [17, 18]. These quadrupolar effects encode the fact that the object has finite size. The last term contains dissipative effects [7, 8] due to the internal structure of the stellar object with \tilde{O}_E a composite operator that represent leading order additional degrees of freedom of the object.

We can ensure that our theory will be predictive by expanding our action in a small ratio of parameters v/c ,

ℓ/r and Ω/Ω_0 to the desired accuracy. The scales, ℓ , the radius of the object and Ω_0 , the typical frequency, do not appear explicitly in the action but determine the characteristic size of the dimensionful coupling constants. The tower of higher order spin terms is under control as long as the rotational velocity is much less than the speed of sound c_s of the material in the star, $\Omega \ell \ll c_s$ [5]. For a star, this rotational frequency would be such that the body would undergo large non-linear stresses and order one distortions, breaking down the theory. We evolve the systems until there is a collision or a disruption of one of the objects. For an equal mass BBH with orbital separation r , the expansion $\ell/r \sim 1/2$ at collision, which means that in order to create accurate templates higher order terms in the expansion are to be included in the numerical framework.

A. Newtonian Dynamics

We start by taking the Newtonian limit of our effective action $C_{0i0j} \approx \partial_i \partial_j \Phi$, $d\tau \approx dt \sqrt{1 + 2\Phi - \dot{\vec{y}}^2}$ with y the location of the star, Φ the Newtonian potential, and $\Omega^i = \frac{1}{2} \epsilon^{ijk} \mathcal{R}_{jl} \partial_l \mathcal{R}_k^i$ with $\mathcal{R}(\theta^i)$ a rotation matrix [8]. The action then reads

$$\begin{aligned} S = \int dt \left\{ \frac{mv^2}{2} - m\Phi + \frac{I}{2} \Omega_i \Omega^i + \frac{n_{\Omega}}{2} \Omega^i \Omega^j \partial_i \partial_j \Phi \right. \\ \left. + \frac{n_E}{4} \partial^i \partial^j \Phi \partial_i \partial_j \Phi + \frac{n'_E}{4} \partial^i \partial^j \dot{\Phi} \partial_i \partial_j \dot{\Phi} \right. \\ \left. + \frac{1}{2} \partial_i \partial_j \Phi \mathcal{R}_k^i \mathcal{R}_l^j \mathcal{O}_E^{kl} \right\} \quad (3) \end{aligned}$$

We obtain the equations of motion by using a modified variation [19] to account for dissipative effects [8]. Varying with respect to x^i and θ^i yields

$$\begin{aligned} m\dot{v}_i = -m\partial_i \Phi + \frac{n_{\Omega}}{2} \Omega^k \Omega^j \partial_i \partial_j \partial_k \Phi \\ + \frac{n_E}{2} \partial_i \partial_j \partial_k \Phi \partial^j \partial^k \Phi + \frac{n'_E}{2} \partial_i \partial_j \partial_k \dot{\Phi} \partial^j \partial^k \dot{\Phi} \\ - \frac{\eta_E}{2} \partial_i \partial_j \partial_k \Phi (\partial^j \partial^k \dot{\Phi} + 2\partial^j \partial_l \Phi \epsilon^{klm} \Omega_m) \quad (4) \end{aligned}$$

for the acceleration of the compact object and

$$\begin{aligned} \partial_t (I\Omega^i + n_{\Omega} \Omega^j \partial_i \partial_j \Phi) = -n_{\Omega} \epsilon_{ijk} \Omega^k \Omega^l \partial^j \partial_l \Phi \\ + \eta_E \partial^j \partial^k \Phi (3\partial_i \partial_j \Phi \Omega_k - 2\partial_j \partial_k \Phi \Omega_i + \epsilon_{ikl} \partial^l \partial_j \dot{\Phi}) \quad (5) \end{aligned}$$

for the change of rotational angular momentum with contribution from n_{Ω} and η_E . By substituting the Newtonian potential Φ and restricting the spin Ω_i to be aligned to the orbital plane for simplicity, we obtain

$$\begin{aligned}
m_1 \dot{\vec{v}} = & -\frac{Gm_1 m_2 \hat{r}}{r^2} - \frac{3n_\Omega G m_2 \Omega^2 \hat{r}}{2r^4} - \frac{9n_E G^2 m_2^2 \hat{r}}{r^7} \\
& - \frac{9\eta_E G^2 m_2^2}{r^8} (\vec{r} \times \vec{\Omega} + \vec{v} + 2\hat{r}(\hat{r} \cdot \vec{v})) \quad (6) \\
& - \frac{18n'_E G^2 m_2^2}{r^9} (2v^2 \hat{r} + 5(\hat{r} \cdot \vec{v})^2 \hat{r} - \vec{v}(\hat{r} \cdot \vec{v}))
\end{aligned}$$

and

$$\begin{aligned}
& \left(I + \frac{Gm_2 n_\Omega}{r^3} \right) \partial_t \vec{\Omega} \\
= & \frac{3Gm_2 n_\Omega (\hat{r} \cdot \vec{v}) \vec{\Omega}}{r^4} + \frac{9\eta_E G^2 m_2^2}{r^7} (\hat{r} \times \vec{v} - r \vec{\Omega}). \quad (7)
\end{aligned}$$

We now have our equations of motion that are to be integrated numerically.

1. Neutron Stars

We first introduce the Newtonian tidal disruption distance for a NS in a binary with a BH, $r_r \approx \ell_\star (m_\bullet/m_\star)^{1/3}$ [20] with m_\bullet and m_\star the mass of the BH and of the NS respectively and ℓ_\star the radius of the NS. This scale sets when the disruption of the star will happen. At this distance, roughly half of the object will no longer be bound to itself and will be bound to the BH. Although additional corrections need to be taken into account for a better description of the disruption, for the purpose of this work the Newtonian disruption term is enough.

The moment of inertia for a NS can be approximated as [21]

$$I = 0.21 \frac{m\ell^2}{1 - 2Gm/\ell c^2} \quad (8)$$

where m and ℓ are the mass and radius of the NS. The speed of sound inside the star is $c_s \lesssim c/\sqrt{3}$ [22]. To take into account tidal effects we make use of the Love number n_E for NSs. The spin coefficient n_Ω in the Newtonian limit $n_\Omega = n_E$ [23]. The coefficients n_E and n'_E are obtained from [6] for a NS with $m = 1.2M_\odot$, $\ell = 8.89km$ and polytropic index 1, by looking at the response function in terms of the frequencies and overlap integrals of the fundamental mode of the star. The response function reads

$$\begin{aligned}
\mathcal{F}(\tilde{F}) = & \frac{1}{2} \frac{\ell^5}{G} \frac{q_f^2}{\ell^2(\omega_f^2 - \omega^2)/c^2} \\
= & \frac{1}{2} \frac{\ell^5}{G} \frac{q_f^2}{\ell^2\omega_f^2/c^2} \left(1 + \frac{\omega^2}{\omega_f^2} + \dots \right) \quad (9)
\end{aligned}$$

where we have expanded over ω/ω_f with ω_f the fundamental frequency of the star. The overlap integral of the

fundamental mode q_f [24] is dimensionless as well as the combination $\ell\omega_f/c$. We identify the Love coefficient

$$n_E = \frac{1}{2} \frac{\ell^5}{G} \frac{q_f^2}{\ell^2\omega_f^2/c^2} \quad (10)$$

and comparing to the Newtonian tidal coefficient $n_E = 2k\ell^5/3G$ [8] we identify the dimensionless Love number k computed using the Lane-Emden Equation [25]

$$k = \frac{3}{4} \frac{q_f^2}{\ell^2\omega_f^2/c^2} \quad (11)$$

From the above expansion of the response function, the term n'_E reads

$$n'_E = \frac{1}{2} \frac{\ell^7}{Gc^2} \frac{q_f^2}{\ell^4\omega_f^4/c^4} = \frac{1}{2} \frac{\ell^7}{Gc^2} k' \quad (12)$$

for a limit in which $\omega/\omega_f \ll 1$. We have defined k' as the dimensionless part of n'_E and found $k' = 1.1311$.

The coefficient regarding dissipative effects in NSs is unknown and is to be matched from hydrodynamical numerical simulations.

2. Black Holes

The radius for a Schwarzschild BH is $\ell_s = 2GM/c^2$ while for the Kerr BH $\ell_\pm = (\ell_s \pm \sqrt{\ell_s^2 - 4S^2})/2$ with $S = J/(Mc)$ the BH specific angular momentum radius and $J = I\Omega$ the scalar value of the BH angular momentum. The moment of inertia of the outer radius for a rotating BH reads $I_+ = M\ell_+^2$. The Love numbers for BHs within general relativity are expected to be zero [18, 26]. The theoretical value of the response function for dissipative effects in non rotating black holes has been computed in [7], from which we obtain η_E

$$\eta_E = \frac{16}{90} \frac{G^5 M^6}{c^{13}} = \frac{\ell_s^6}{360Gc} \quad (13)$$

with M the mass of the black hole.

In the spinning case, η_E is a function of l_+ and there exists an additional dissipative coefficient η_Ω that is different from η_E [26], but our numerical implementation does not allow us to take it into account. For illustrative purposes, we make use only of the dissipative coefficient η_E , for both non-spinning and spinning case.

B. Non-Relativistic General Relativity

1. Post-Newtonian Dynamics

Non-Relativistic General Relativity was introduced in [9] to calculate the post-Newtonian expansion and since

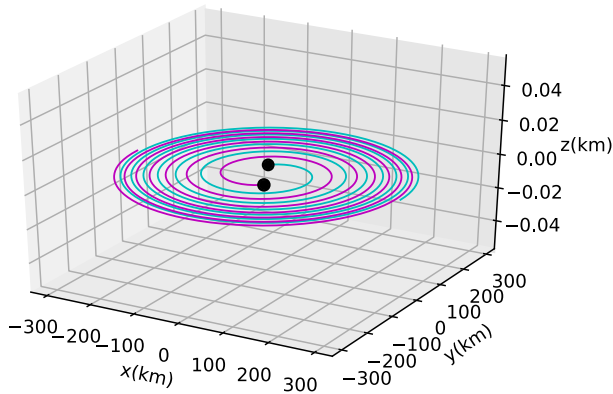


FIG. 1. The late inspiral evolution of an equal mass BBH with $M = 20M_{\odot}$ and initial orbital distance of $d = 10\ell_{\bullet}$. The simulation runs until there is a collision. The system decays due to GW radiation by including the leading order 2.5 PN term.

then many tools have been developed within this framework, such as the ones we have implemented. For a thorough review of the theory of the PN expansion in EFT see [27, 28]. From the EFT perspective we can obtain the PN corrections from each of the terms in the action. We make use of the PN expansion to the point particle term. The PN corrections for the non-spinning case can be expanded in a series as

$$\vec{a} = \vec{a}_{\star} + c^{-2}\vec{a}_2 + c^{-4}\vec{a}_4 + c^{-5}\vec{a}_5 + \mathcal{O}(c^{-6}) \quad (14)$$

where a_{\star} is the acceleration which includes all the Newtonian effects of the star. The terms \vec{a}_2 and \vec{a}_4 account for the periastron shift. The leading order term that accounts for radiation of energy and momentum through GW is the 2.5 PN term [9, 29]

$$\vec{a}_5 = \frac{4}{5} \frac{G^2 m_1 m_2}{r^3} \left[\left(\frac{2Gm_1}{r} - \frac{8Gm_2}{r} - v^2 \right) \vec{v} + (\hat{r} \cdot \vec{v}) \left(\frac{52Gm_2}{3r} - \frac{6Gm_1}{r} + 3v^2 \right) \hat{r} \right] \quad (15)$$

For the rest of the paper we make use of the modified acceleration $\vec{a} = \vec{a}_{\star} + c^{-5}\vec{a}_5$. The GW decay due to the 2.5 PN term is shown in figure 1 for an equal mass BBH.

2. Spinning Objects

In principle, the equations of motion from the Spin-Orbit and Spin-Spin coupling contributes to the phase evolution at lower order than the spin effects that we have already included, but the ones obtained in [30–33] are not unique and they depend on a condition to the spin, which is related to the definition of the center of mass worldline for each body. This gauge fixing is used

to remove fictitious degrees of freedom from a relativistic angular momentum S_{ab} as in [30, 32]. From the model we are using based on the corset, there is no need to impose additional constraints on the angular velocity Ω^{cd} because it has already been gauge fixed [8]. To obtain the equation of motion of these terms would require more work and for the purposes of this work we do not compute it nor implement it numerically.

III. NUMERICAL SIMULATIONS

A. Point Particle Simulations Plus Corrections

1. Position, Velocity and Acceleration

We implement a 4th order Hermite integrator [4, 34]. In the point particle approximation, the predicted values of the position, velocity and acceleration for the next step are obtained from

$$\begin{aligned} \vec{r}_{i+1} &= \vec{r}_i + \vec{v}_i \Delta t + \frac{1}{2!} \vec{a}_i \Delta t^2 + \frac{1}{3!} \vec{j}_i \Delta t^3 + \dots \\ \vec{v}_{i+1} &= \vec{v}_i + \vec{a}_i \Delta t + \frac{1}{2!} \vec{j}_i \Delta t^2 + \dots \\ \vec{a}_{i+1} &= \vec{a}_i + \vec{j}_i \Delta t + \dots \end{aligned} \quad (16)$$

where $\vec{j} = \dot{\vec{a}}$, by computing the force calculation as

$$\begin{aligned} \vec{a}_i &= \frac{Gm_2 \hat{r}}{r^2} \\ \vec{j}_i &= \frac{Gm_2}{r^3} \{ \vec{v} - 3(\vec{v} \cdot \hat{r}) \hat{r} \} \end{aligned} \quad (17)$$

with the position and velocity from the previous step. The force calculation \vec{a}_{i+1} and \vec{j}_{i+1} is done using the predicted values \vec{r}_{i+1} and \vec{v}_{i+1} to get the corrected position, velocity and acceleration

$$\begin{aligned} \vec{r}_{i+1,c} &= \vec{r}_i + \frac{1}{2}(\vec{v}_i + \vec{v}_{i+1})\Delta t + \frac{1}{12}(a_i - \vec{a}_{i+1})\Delta t^2 \\ \vec{v}_{i+1,c} &= \vec{v}_i + \frac{1}{2}(\vec{a}_i + \vec{a}_{i+1})\Delta t + \frac{1}{12}(\vec{j}_i - \vec{j}_{i+1})\Delta t^2 \\ \vec{a}_{i+1,c} &= \vec{a}_i + \frac{1}{2}(\vec{j}_i + \vec{j}_{i+1})\Delta t \end{aligned} \quad (18)$$

up to the jerk correction. With this very simple framework we are capable of numerically evolving our theory, obtaining the desired accuracy by using a specific time-step Δt . The same algorithm applies for all other Newtonian terms and PN effects that we have considered. It is just necessary to include them in (17).

2. Spin evolution

We solve for the angular velocity $\vec{\Omega}$ in a similar fashion as above. We define $\vec{b} = \partial_t \vec{\Omega}$ and correct the angular velocity

$$\vec{\Omega}_{i+1,c} = \vec{\Omega}_i + \frac{1}{2}(\vec{b}_i + \vec{b}_{i+1})\Delta t + \frac{1}{12}(\dot{\vec{b}}_i - \dot{\vec{b}}_{i+1})\Delta t^2 \quad (19)$$

B. Matching of Coefficients and Numerical Tests

Many Newtonian and PN high precision numerical codes within this approach have been implemented to do numerical experiments. Testing the Newtonian limit is straightforward. To test the PN corrections we use the GW time decay [35] which has been a useful test of many implementations, i.e [36]. The finite time T_m for the decay of a binary in a circular orbit reads

$$T_m(d) = \frac{5}{256} \frac{d^4 c^5}{G^3 m_1 m_2 (m_1 + m_2)} \quad (20)$$

with d the orbital distance of the binary.

To test the rest of the effects we can match the coefficients of the theory from the corrected position, velocity and acceleration at each time-step. This testing approach puts tight bounds on the accuracy of the simulation. From an EFT perspective, we can follow the energy hierarchy to measure different coefficients. Consider for instance a BH-NS binary without any spin and neglect for a moment the PN effects. The dynamics of the NS will change due to the tidal effects, and the matching of coefficients reads

$$n_E = \frac{r^5 m_1}{9Gm_2} \left(\frac{a_{*,j}}{a_{N,j}} - 1 \right) \quad (21)$$

where $a_{N,j}$ is one of the spatial components of the Newtonian term ($j = \{x, y, z\}$), as well as for $a_{*,j} = a_{N,j} + a_{T,j}$ the acceleration of the star due to all effects with $a_{T,j}$ being the acceleration due to tides. Thus if we solve our system in the $x - y$ plane with these coordinates, we are to match to coefficient for each spatial component. Then we add the PN effects and measure the coefficient as

$$n_E = \frac{r^5 m_1}{9Gm_2} \left(\frac{a_{*,j}}{a_{N,j}} - \frac{a_{PN,j}}{a_{N,j}} - 1 \right) \quad (22)$$

The matching of coefficients from tidal effects is the simplest, but we can add all effects and go order by order in the energy hierarchy to measure the coefficients and test the implementation. Figure 2 shows the time evolution measurement of the static tidal coefficient from a numerical simulation of a BH-NS coalescence.

Although we do not compare the late inspiral dynamics with numerical relativity, we test our code by matching the coefficients and make use of the fact that previous work [11] with similar high precision numerical schemes has shown to be predictive in the late inspiral regime, up to the very last few orbits. We also comment that the

comparison of EFT simulations with numerical relativity is still very unexplored, but we hope this work motivates for the building up of high precision codes that can match numerical relativity simulations. We also hope to illustrate the matching of coefficients from numerical simulations in order to compare our predicted values from stellar perturbations with our state of the art hydrodynamical simulations and to match the coefficients from GW observations in the near future.

C. Waveforms

We systematically add the Newtonian effects and extract the lowest order gravitational waveform for different systems. The GW amplitude for an inspiral binary in a quasi-circular orbit reads [37]

$$h_+(t) = \frac{1}{r_o} \frac{4G\mu\omega_s^2 d^2}{c^4} \left(\frac{1 + \cos^2 \iota}{2} \right) \cos(2\omega_s t) \quad (23)$$

where $\mu = m_1 m_2 / (m_1 + m_2)$ is the reduced mass of the system, and r_o is the distance from the observer to the system. The orbital frequency $\omega_s^2 = G(m_1 + m_2) / d^3$ from Kepler's law. If we see the orbit edge-on, $\iota = \pi/2$, then h_\times vanishes and the GW is linearly polarized, at $\iota = 0$, h_+ and h_\times have the same amplitude. For simplicity we take $\iota = \pi/2$ to systematically compare waveforms of binaries with different effects in their late inspiral. We have chosen an arbitrary r_o which makes the system detectable in the LIGO-Virgo band.

In the next subsections we describe the implementation and show the contribution to the phase evolution for different binaries due to the additional Newtonian effects in the numerical simulations. Each binary is set with initial conditions of a Newtonian circular orbit at the chosen initial distance.

1. Oscillations in Black Hole-Neutron Star Interactions

To study the effects of tides in the late inspiral we perform three numerical simulations of a NS-BH binary $m_\bullet = 5M_\odot$, $m_\star = 1.2M_\odot$ and $\ell_\star = 8.89km$ with same initial conditions at a distance of $10\ell_\star$ but differing in the effects that the simulations includes: PN, static and dynamical tides. The simulation is finished when the star is disrupted in the Newtonian limit at r_τ . We have chosen the size of the black hole so that the star disrupts just outside the horizon. In figure 3 we compare the phase evolution in the waveforms from a binary with different effects: PN, PN + static tides and PN + dynamical tides. Tidal effects have a significant contribution to the phase evolution making the system to merge faster. Static tides enter at lower order than the dynamical part, and thus have a bigger impact in the phase evolution. Nevertheless, the dynamical part that enters at higher order also has a significant contribution. Thus, for the equation of

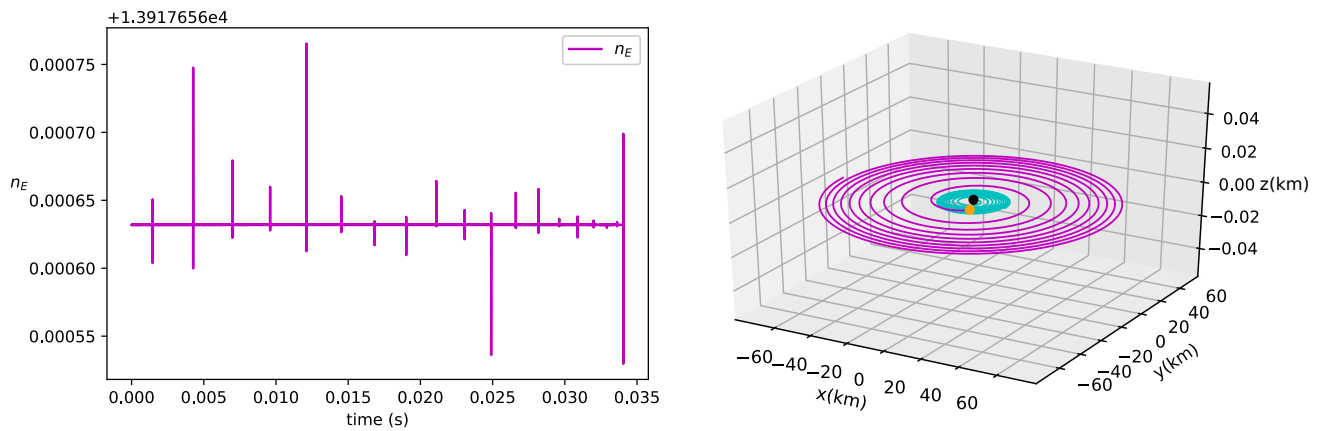


FIG. 2. Measurement of the tidal coefficient n_E in a simulation of a BH-NS coalescence. On the left figure the coefficient n_E is measured at each time-step of the simulation for a fixed time-step of $dt = 0.001$ in code units. The theoretical value of the coefficient for the NS used is $n_{E,t} = 13917.65663191198$ and is measured with an accuracy of $n_E/n_{E,t} \sim 10^{-8}$. The figure on the right illustrates the trajectories followed by the binary with initial separation of $d = 10\ell_*$ until the disruption of the NS at r_τ just outside the horizon.

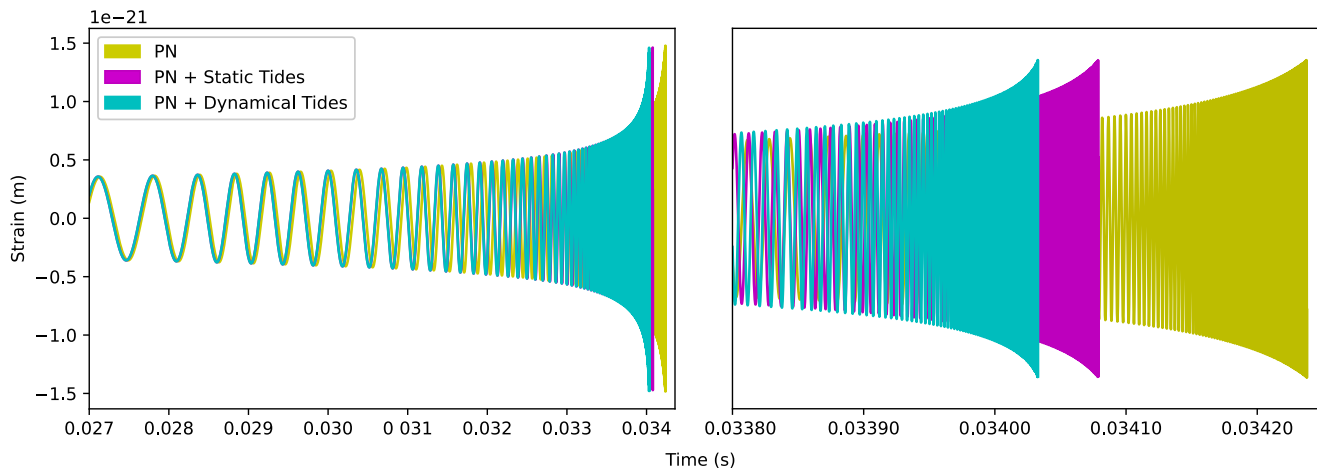


FIG. 3. The GW template from the late inspiral of a BH-NS coalescence. Each waveform color is extracted from simulations with different effects. The lime waveform is only PN, the magenta is PN + Static Tides and the cyan is PN + Dynamical Tides. Tides contribute to the phase evolution making the system merge faster. The Newtonian static and dynamical tidal effects have a significant contribution that should be measurable from observations in order to match the coefficients of the theory.

state of the NS used in our simulations, the matching of coefficients of the response function from gravitational wave observations might be possible. This matching can place tighter bounds on the equation of state of matter for NSs, compared to only constraining the static Love number [12], and a detailed analysis as in [13] needs to be done to actually put accurate bounds on our model.

2. Dissipation in Black Hole Mergers

We have performed simulations for two different cases in order to compare the effects due to dissipation. We run an equal mass case $q = m_1/m_2 = 1$ with $m_2 =$

$20M_\odot$ and initial distance of $10\ell_*$. The second case is an unequal mass binary with $q = 1/2$ and $m_2 = 40M_\odot$ and initial distance $r = 8\ell_{*,2}$, the radius of the bigger black hole. The gravitational waveforms are shown in figure 4. Dissipative effects in the late inspiral of a black hole binary have a minor role on changing the waveform compared to tides by slightly contributing to the phase evolution. The comparison of both plots shows that if we are to measure the dissipative coefficient from black hole interactions, we should do it from an unequal mass case. The matching of this coefficient will allow us to learn about the nature of black holes and thus about gravity.

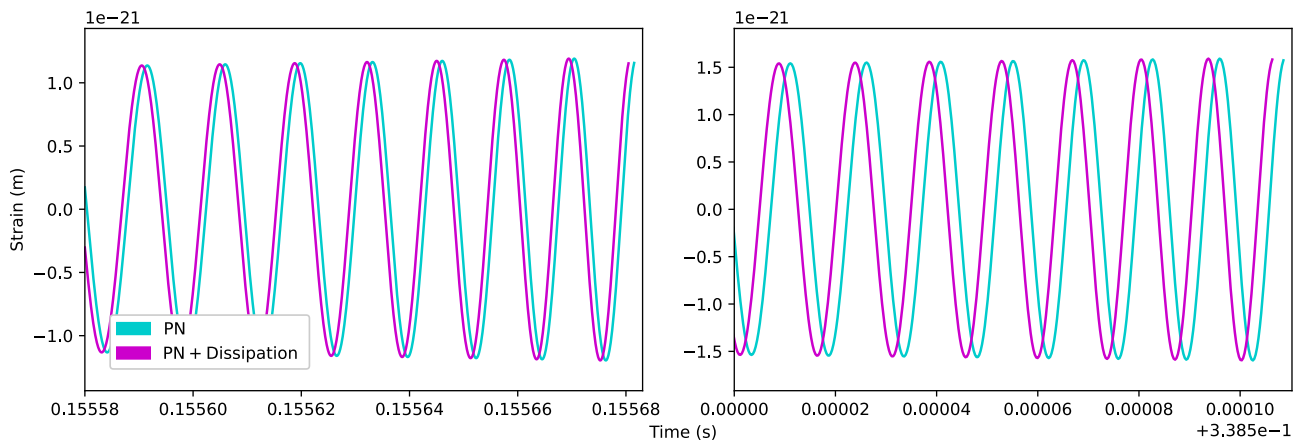


FIG. 4. The gravitational waveform from the late inspiral of a BBH that contains dissipative effects. On the left figure we have the comparison of waveforms in the late inspiral with PN and PN + Dissipation from an equal mass $q = m_1/m_2 = 1$ binary with $m_\bullet = 20M_\odot$ and an initial distance of $d = 10\ell_\bullet$. The figure on the right is the comparison of waveforms from an unequal mass BBH with $q = 1/2$, $m_2 = 40M_\odot$ and $d = 8\ell_{\bullet,2}$. The contribution of dissipative effects to the phase evolution is less compared to tidal effects and it is better to measure the coefficients from an unequal mass system.

3. Spinning Objects

We have restricted the spin of the compact object to be aligned with the orbital angular momentum. In order for our theory to work appropriately, we choose the dimensionless spin $\vec{\chi}$ of the object

$$\vec{\chi} = \frac{\vec{J}_c}{GM^2} \quad (24)$$

to be slow and non negligible $0 < \chi \ll 1$ in order to have an effect in the simulations but not to break down the theory. We add slow spin to both previous cases.

Thus, we add spin $\chi = [0.1, 0.2]$ to the NS in the BH-NS system with same initial conditions as before and find in figure 5 that the spin correction due to gravity have a significant contribution to the phase evolution, making the system to merge faster. We also note that even though the spin contribution enters at lower order in the equations of motion, its contribution is smaller compared to the tidal effects, given that we have a model for slowly spinning particles. The spin evolution of the NS is negligible for the evolved time. For BHs, there is no spin correction given that the spin coefficient is zero [26] and the contribution of the spin in the dissipative effects is insignificant for the time evolved. Thus, there is no change in the waveform on the BBH coalescence due to the added spin effect.

4. Spinning Neutron Star Binaries

We set an equal mass NS-NS binary with initial distance of $d = 8\ell_\star$ and evolve the system until there is a

collision. We run four different simulations that includes PN, dynamical tides and aligned spin $\chi = 0.1$ to the NSs in order to illustrate different scenarios, which are shown in figure 6. Each spinning star contributes equally to the phase evolution with the spin. Tidal effects have a greater role in the phase evolution than spin, even though they appears at higher order in the action. This is because we are dealing with slowly spinning objects and thus the contribution from $\vec{\Omega}$ into the dynamics is also small.

IV. DISCUSSION

In this work we have implemented the numerical evolution of the late inspiral of compact objects within the EFT framework using a high accuracy 4th order Hermite integrator for point particle simulations. We have successfully added into the dynamics leading order Newtonian spin, tidal and dissipative effects plus the 2.5 PN corrections due to GW radiation. We have tested our implementation by matching the coefficients of the effective theory at each time-step from the numerical simulations and showed the overall phase evolution of the waveform due to each effect. This is the first step towards constructing realistic models in the late inspiral that are computationally cheap and accurate by adding higher order correction terms beyond the PN expansion. This numerical framework can allow us to create a rich template bank of waveforms for different classes of stars and systems.

Matching the coefficients of the effective theory from observations will have profound implications on our understanding of fundamental physics. By properly matching the tidal coefficients of the response function of a NS in a NS-BH or a NS-NS interaction from GW obser-

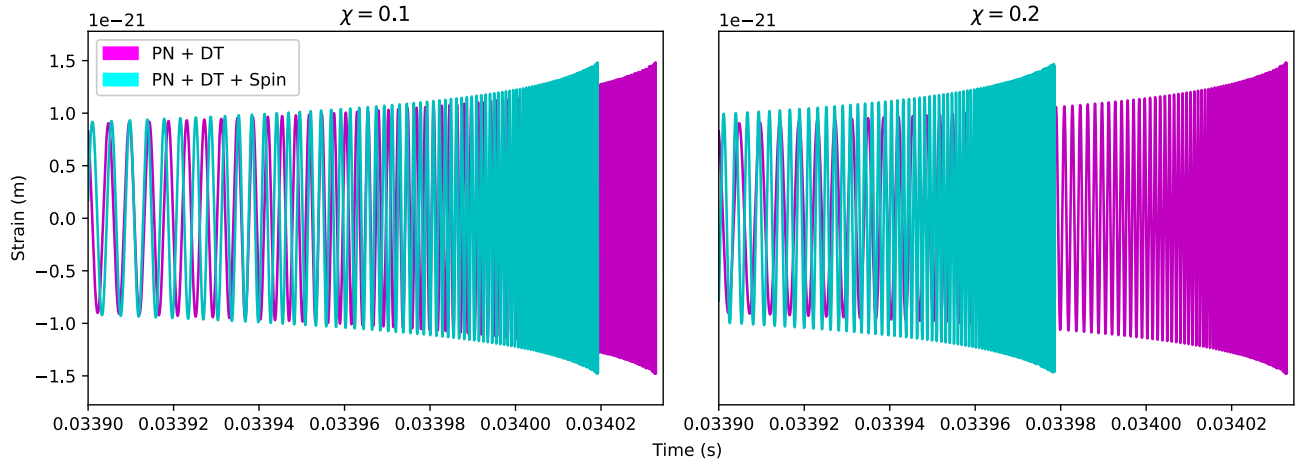


FIG. 5. Overall phase evolution due to the spin corrections in addition to the dynamical tides (DT) in the late inspiral of a BH-NS binary. We add aligned spin to the NS and use same initial conditions as for the non-spinning case. In the figure on the left, we have chosen a dimensionless spin of $\chi = 0.1$ and on the right of $\chi = 0.2$. The spin corrections have a significant contribution to the phase evolution that is smaller compared to the contribution from DT.

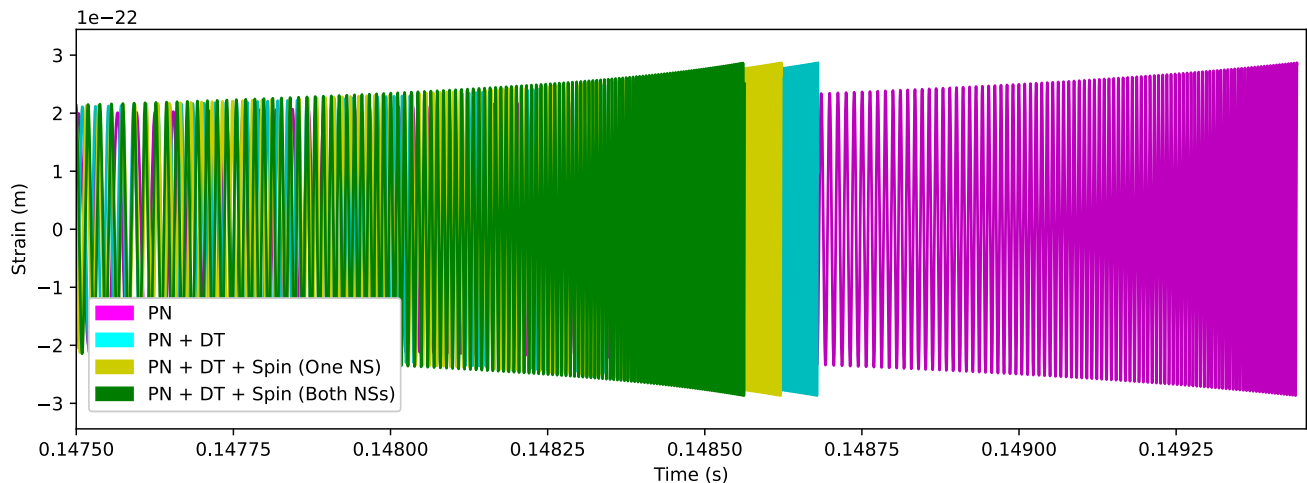


FIG. 6. GWs from four different scenarios of a NS-NS coalescence but same initial conditions at $d = 8l_*$. We add PN, DT and then spin to the NSs, first only to one member and then to both. The spin contribution is smaller than the one from tides given that we are dealing with slowly spinning particles, and each spinning NS contributes equally to the phase evolution.

vations, we can place tight constraints on its equation of state of matter. Although we expect the Love numbers to be zero for BHs in General Relativity, we can learn more about the nature of BHs by measuring its coefficient for dissipative effects. It is also worth noting that for different theories of gravity, tidal effects can be non-zero [38]. In this sense, also, measuring the tidal coefficients for black holes is a test of General Relativity, to possibly find modifications of gravity as an EFT [39].

V. ACKNOWLEDGEMENT

We are extremely grateful to T. Hinderer, L. Heisenberg, J. Samsing, J. Steinhoff, M. Levi, R. Penco, W. Goldberger, L. Lehner, R. Yarza, A. Nishizawa and H. S. Chia for the many enlightening conversations. I.M. is particularly grateful to E. Ramirez-Ruiz, S. Rosswog and S. Nissanke for their support in early stages of the work. This research was supported in part by the National Science Foundation under Grant No. NSF PHY-1748958.

[1] B. Abbott *et al.* (LIGO Scientific, Virgo), Phys. Rev. Lett. **116**, 061102 (2016),

arXiv:1602.03837 [gr-qc].

- [2] B. Abbott *et al.* (LIGO Scientific, Virgo), Phys. Rev. Lett. **119**, 161101 (2017), arXiv:1710.05832 [gr-qc].
- [3] R. Abbott *et al.* (LIGO Scientific, Virgo), (2020), arXiv:2010.14533 [astro-ph.HE].
- [4] P. Hut, J. Makino, and S. McMillan, Astrophys. J. Lett. **443**, L93 (1995).
- [5] L. V. Delacrétaz, S. Endlich, A. Monin, R. Penco, and F. Riva, JHEP **11**, 008 (2014), arXiv:1405.7384 [hep-th].
- [6] S. Chakrabarti, T. Delsate, and J. Steinhoff, Phys. Rev. D **88**, 084038 (2013), arXiv:1306.5820 [gr-qc].
- [7] W. D. Goldberger and I. Z. Rothstein, Phys. Rev. D **73**, 104030 (2006), arXiv:hep-th/0511133.
- [8] S. Endlich and R. Penco, Phys. Rev. D **93**, 064021 (2016), arXiv:1510.08889 [gr-qc].
- [9] W. D. Goldberger and I. Z. Rothstein, Phys. Rev. D **73**, 104029 (2006), arXiv:hep-th/0409156.
- [10] L. Lehner, Class. Quant. Grav. **18**, R25 (2001), arXiv:gr-qc/0106072.
- [11] J. G. Baker, J. R. van Meter, S. T. McWilliams, J. Centrella, and B. J. Kelly, Phys. Rev. Lett. **99**, 181101 (2007), arXiv:gr-qc/0612024.
- [12] E. E. Flanagan and T. Hinderer, Phys. Rev. D **77**, 021502 (2008), arXiv:0709.1915 [astro-ph].
- [13] G. Pratten, P. Schmidt, and T. Hinderer, Nature Commun. **11**, 2553 (2020), arXiv:1905.00817 [gr-qc].
- [14] S. Isoyama and H. Nakano, Class. Quant. Grav. **35**, 024001 (2018), arXiv:1705.03869 [gr-qc].
- [15] A. Maselli, P. Pani, V. Cardoso, T. Abdelsalhin, L. Gualtieri, and V. Ferrari, Phys. Rev. Lett. **120**, 081101 (2018), arXiv:1703.10612 [gr-qc].
- [16] We have explicitly separated dissipative effects from the response function in the action. It can be written as $\mathcal{F}(\bar{F})(\tilde{\omega}) = n_E + i\eta_E \tilde{\omega} + n'_E \tilde{\omega}^2$ [6].
- [17] T. Hinderer, Astrophys. J. **677**, 1216 (2008), arXiv:0711.2420 [astro-ph].
- [18] T. Binington and E. Poisson, Phys. Rev. D **80**, 084018 (2009), arXiv:0906.1366 [gr-qc].
- [19] C. R. Galley, Phys. Rev. Lett. **110**, 174301 (2013), arXiv:1210.2745 [gr-qc].
- [20] M. J. Rees, Nature **333**, 523 (1988).
- [21] D. G. Ravenhall and C. J. Pethick, Astrophys. J. **424**, 846 (1994).
- [22] P. Bedaque and A. W. Steiner, Phys. Rev. Lett. **114**, 031103 (2015), arXiv:1408.5116 [nucl-th].
- [23] K. Yagi and N. Yunes, Phys. Rept. **681**, 1 (2017), arXiv:1608.02582 [gr-qc].
- [24] The overlap integral of the fundamental frequency of the star $q_f = q_{0l}$ in [6].
- [25] E. Poisson and C. Will, *Gravity: Newtonian, Post-Newtonian, Relativistic* (Cambridge University Press, 2014).
- [26] H. S. Chia, (2020), arXiv:2010.07300 [gr-qc].
- [27] R. A. Porto, Phys. Rept. **633**, 1 (2016), arXiv:1601.04914 [hep-th].
- [28] M. Levi, Rept. Prog. Phys. **83**, 075901 (2020), arXiv:1807.01699 [hep-th].
- [29] L. Blanchet, Living Rev. Rel. **9**, 4 (2006).
- [30] R. A. Porto, Phys. Rev. D **73**, 104031 (2006), arXiv:gr-qc/0511061.
- [31] A. Buonanno, G. Faye, and T. Hinderer, Phys. Rev. D **87**, 044009 (2013), arXiv:1209.6349 [gr-qc].
- [32] M. Levi and J. Steinhoff, JHEP **09**, 219 (2015), arXiv:1501.04956 [gr-qc].
- [33] B. A. Pardo and N. T. Maia, (2020), arXiv:2009.05628 [gr-qc].
- [34] J. Makino, M. Taiji, T. Ebisuzaki, and D. Sugimoto, Astrophys. J. **480**, 432 (1997).
- [35] P. C. Peters, Physical Review **136**, 1224 (1964).
- [36] J. Samsing, M. MacLeod, and E. Ramirez-Ruiz, Astrophys. J. **784**, 71 (2014), arXiv:1308.2964 [astro-ph.HE].
- [37] M. Maggiore, *Gravitational Waves. Vol. 1: Theory and Experiments*, Oxford Master Series in Physics (Oxford University Press, 2007).
- [38] V. Cardoso, E. Franzin, A. Maselli, P. Pani, and G. Raposo, Phys. Rev. D **95**, 084014 (2017), [Addendum: Phys.Rev.D 95, 089901 (2017)], arXiv:1701.01116 [gr-qc].
- [39] L. Heisenberg, Phys. Rept. **796**, 1 (2019), arXiv:1807.01725 [gr-qc].